Supplementary information

Bifunctional porphyrin based metal-organic polymers for enhanced electrochemical water splitting

Neidy Ocuane, Yulu Ge, Christian Sandoval-Pauker, Dino Villágran*

*Dino Villagrán

Email: dino@utep.edu

Table of Contents

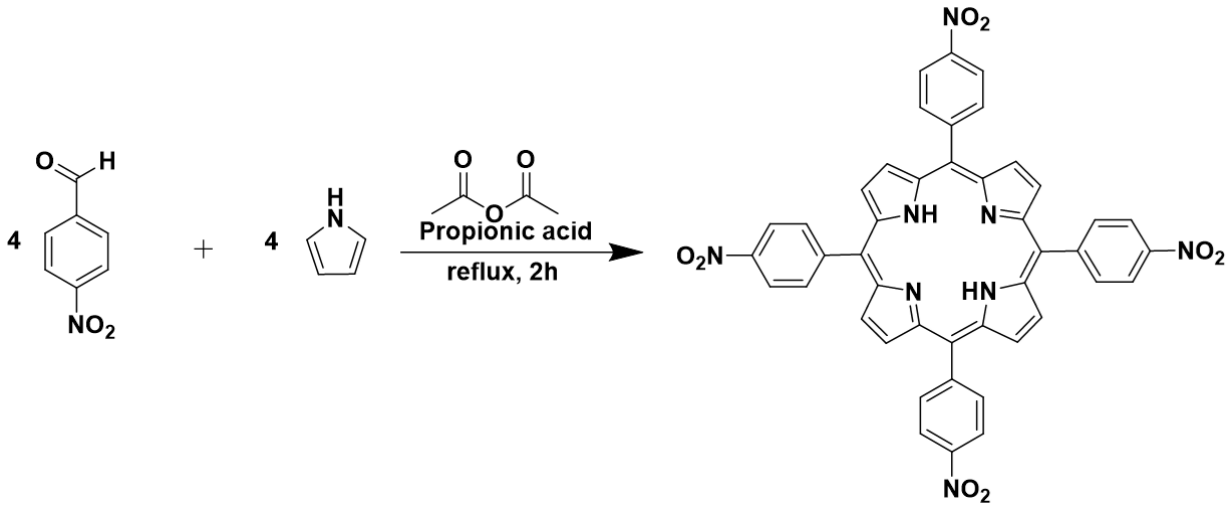

Scheme S1. Synthesis of 5,10,15, 20 tetrakis (4-nitrophenylporphyrin) - H_2TNPP.

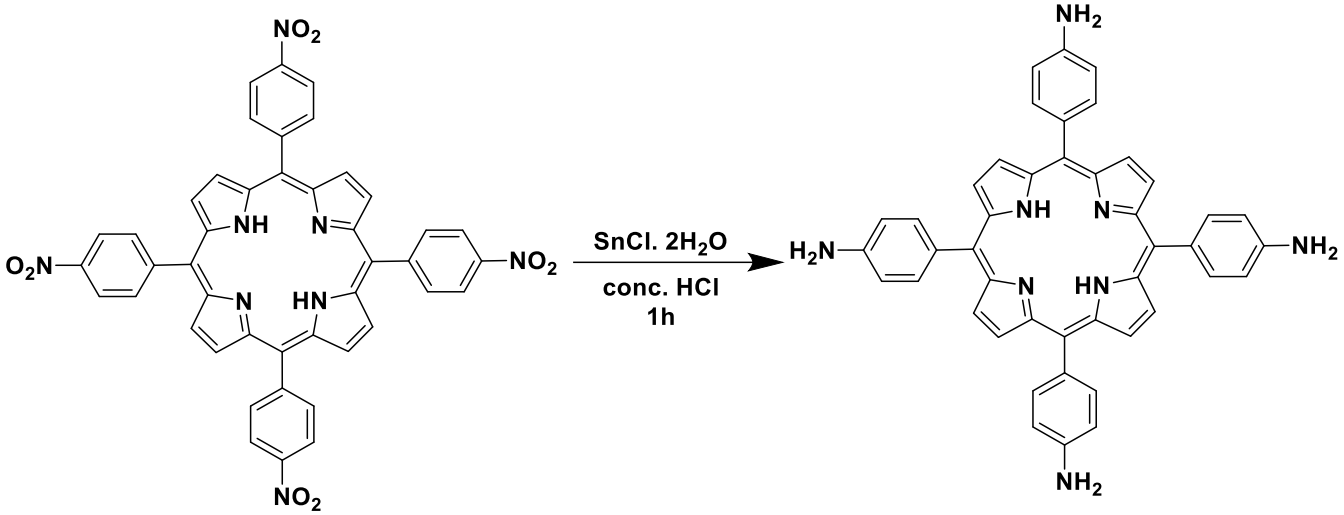

Scheme S2. Synthesis of 5,10,15, 20 tetrakis (4-aminophenylporphyrin) - H_2TAPP.

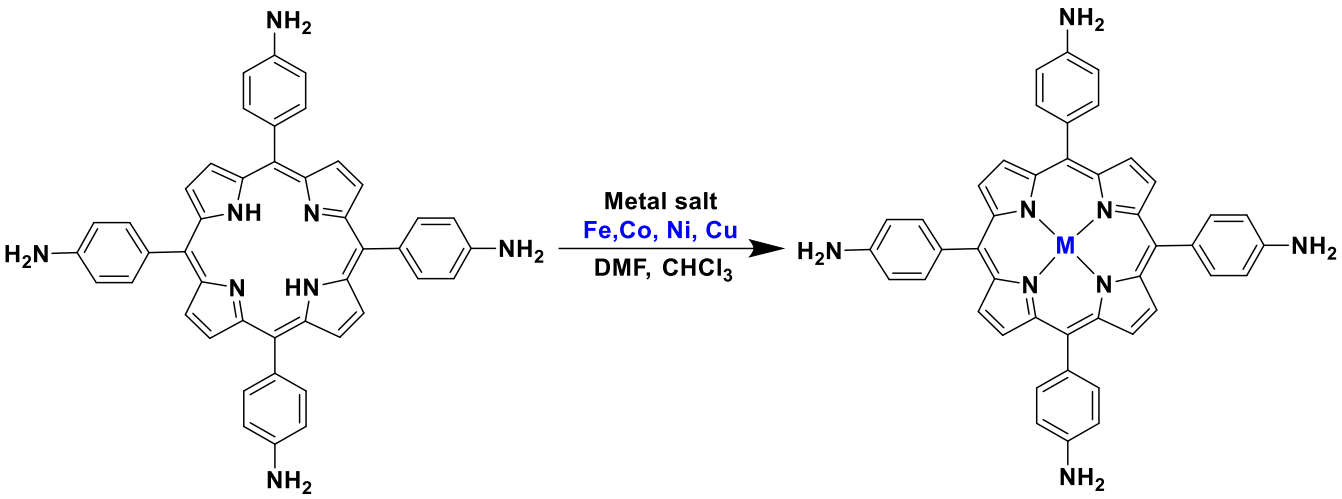

Scheme S3. Synthesis of metalloporphyrin (M-TAPP).

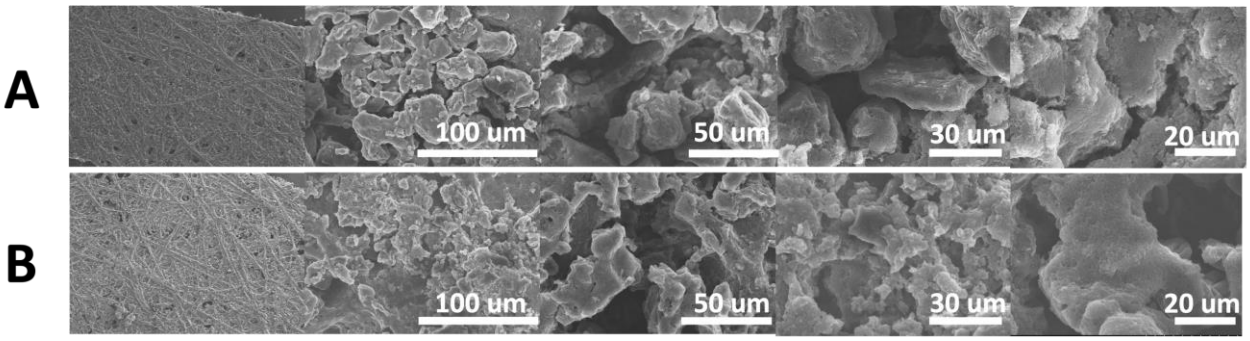

Figure S1: SEM images of carbon paper coated with cobalt polymer **2** ink. A) carbon paper before bulk electrolysis; B) carbon paper electrode after bulk electrolysis.

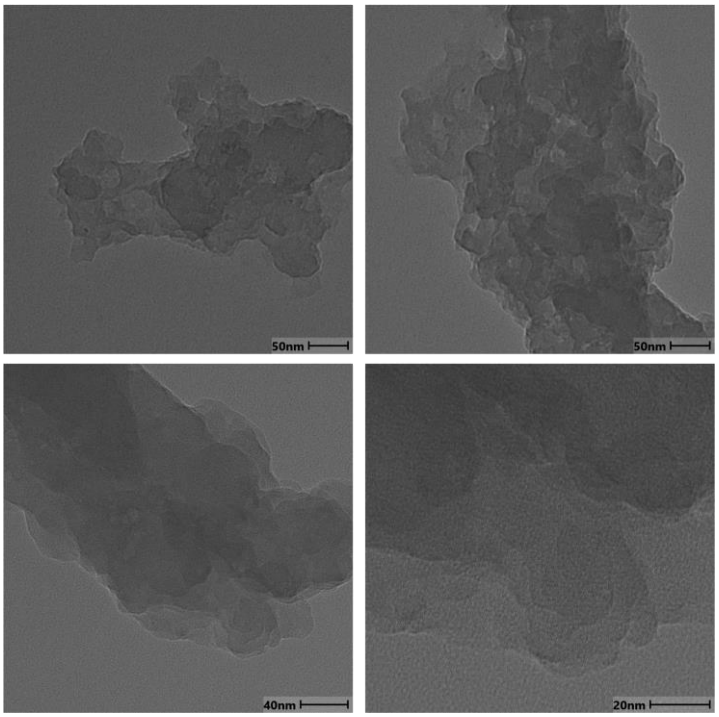

Figure S2: TEM images of cobalt polymer **2**, at different magnifications.

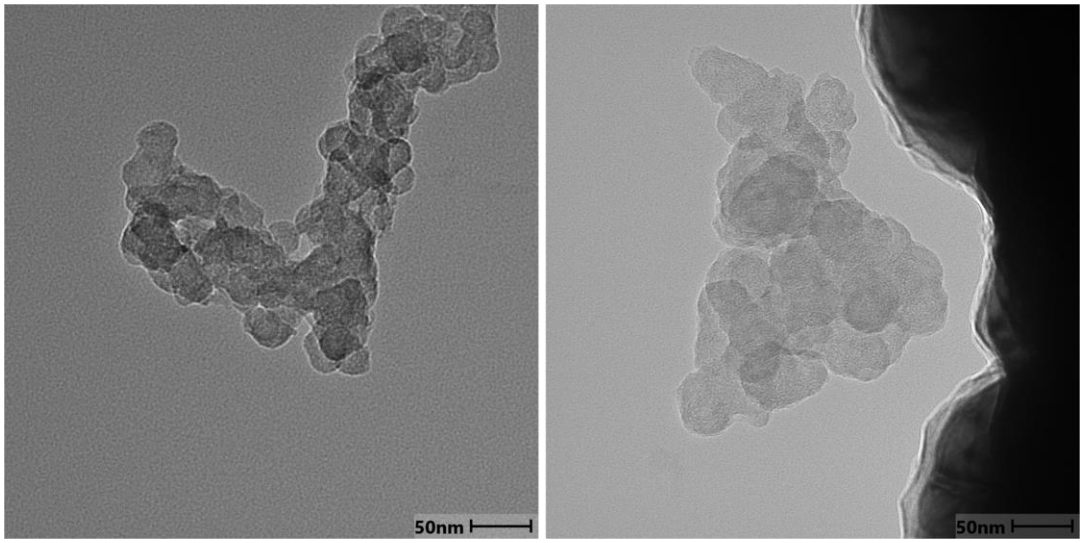

Figure S3: TEM images of polymer **2** after 10h electrolysis experiment in 1M KOH electrolyte solution

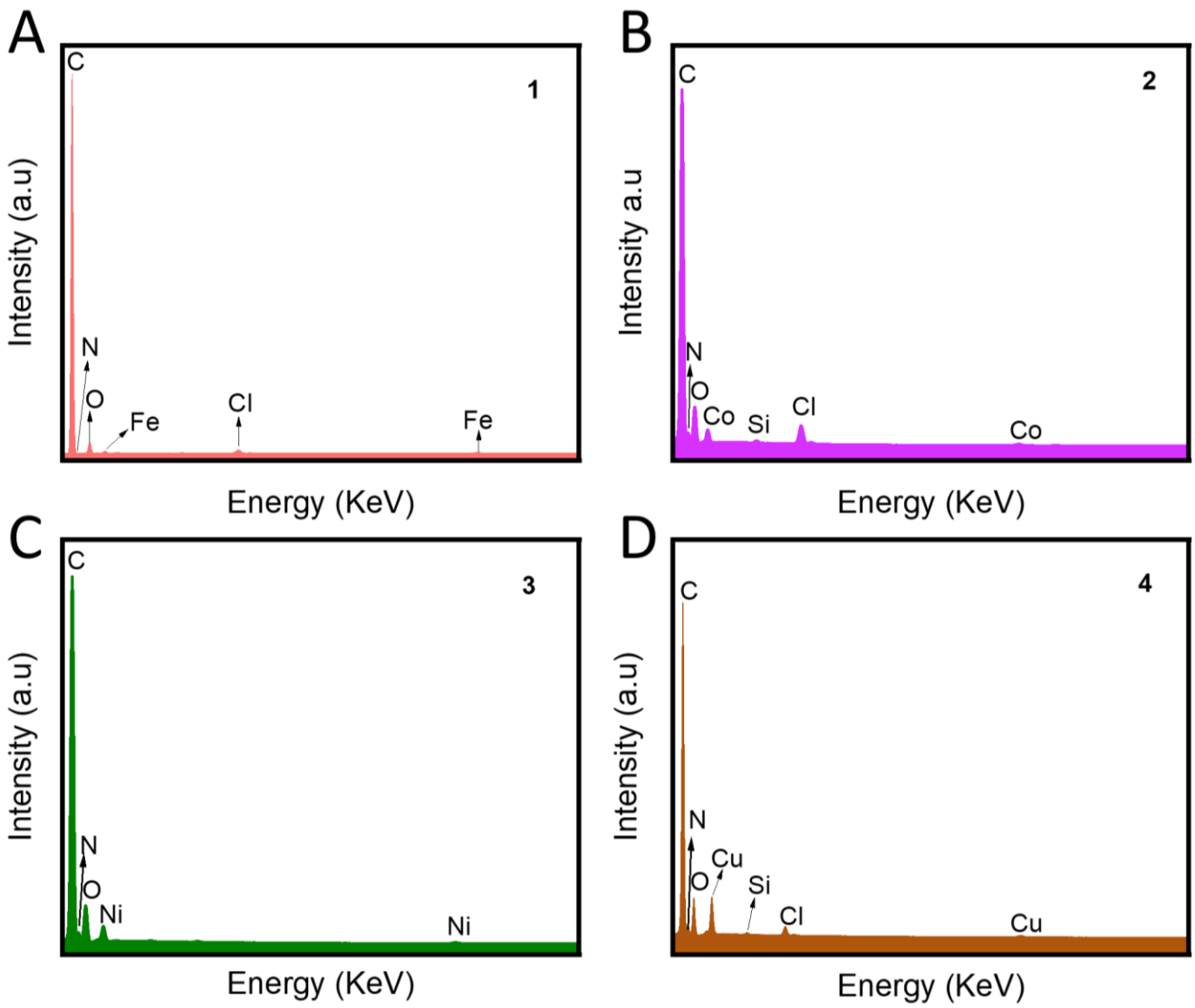

Figure S4. EDX of A) Fe polymer (**1**), B) Co polymer (**2**), C) Ni polymer (**3**), and D) Cu polymer (**4**).

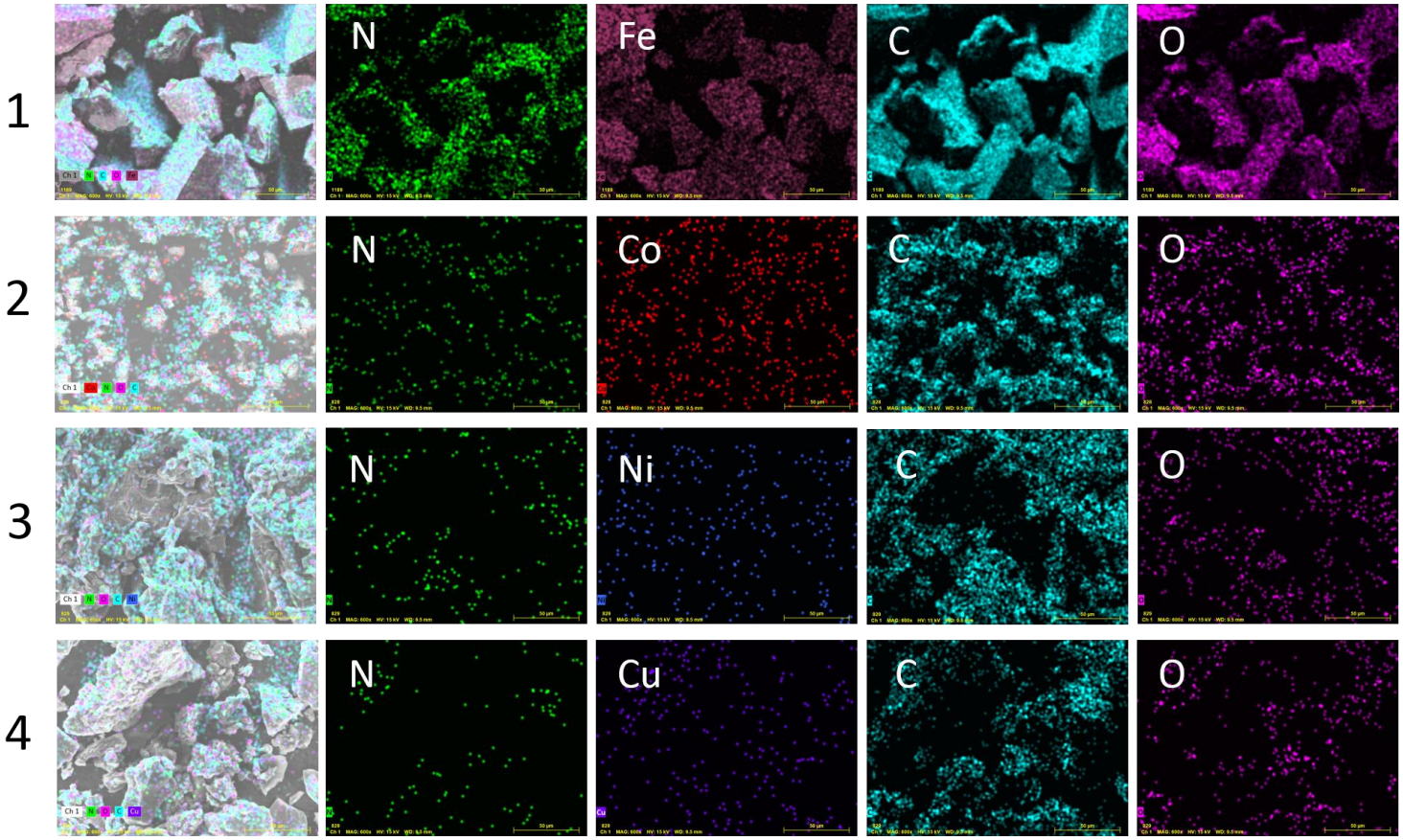

Figure S5. Elemental mapping of Fe polymer (**1**), Co polymer (**2**), Ni polymer (**3**), and Cu polymer (**4**).

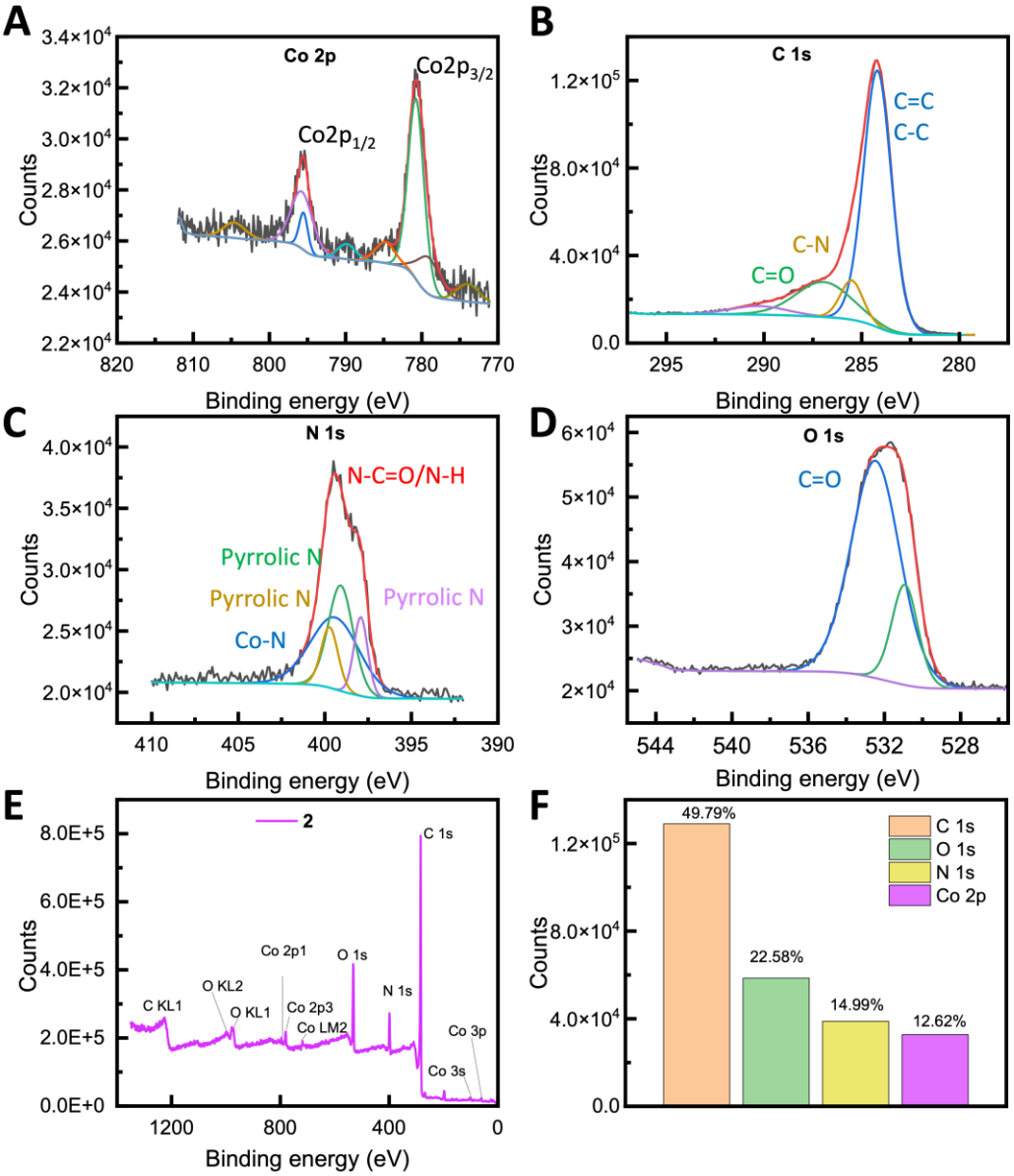

Figure S6: XPS spectra of Co-polymer **2**, (A-D). Full XPS survey (E). Atomic ratio of C, O, N, and Co of polymer **2**.

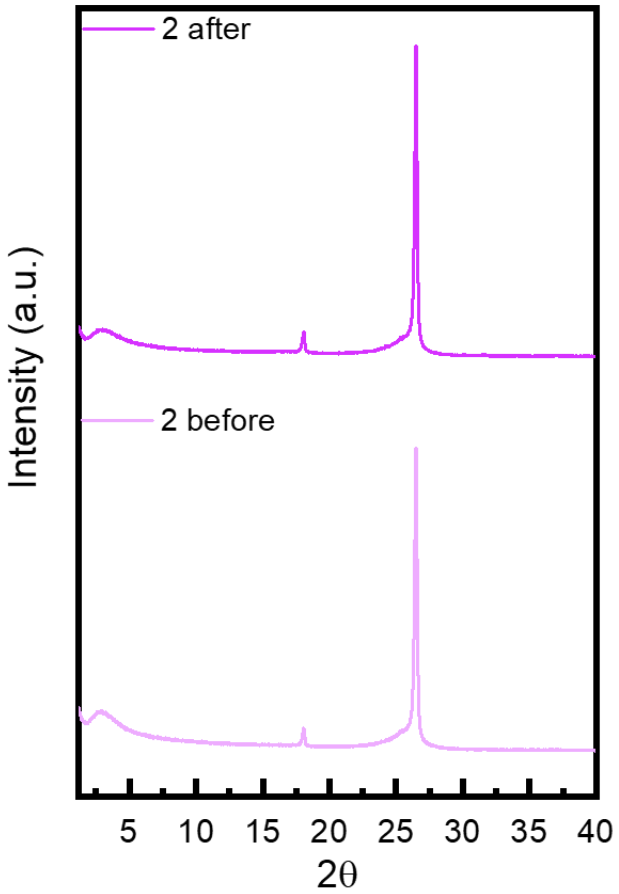

Figure S7: pXRD of the carbon paper electrode coated with cobalt polymer **2**. Bottom diffraction pattern corresponds to the coated electrode before electrolysis and top diffraction pattern corresponds to the spectra after bulk electrolysis experiment.

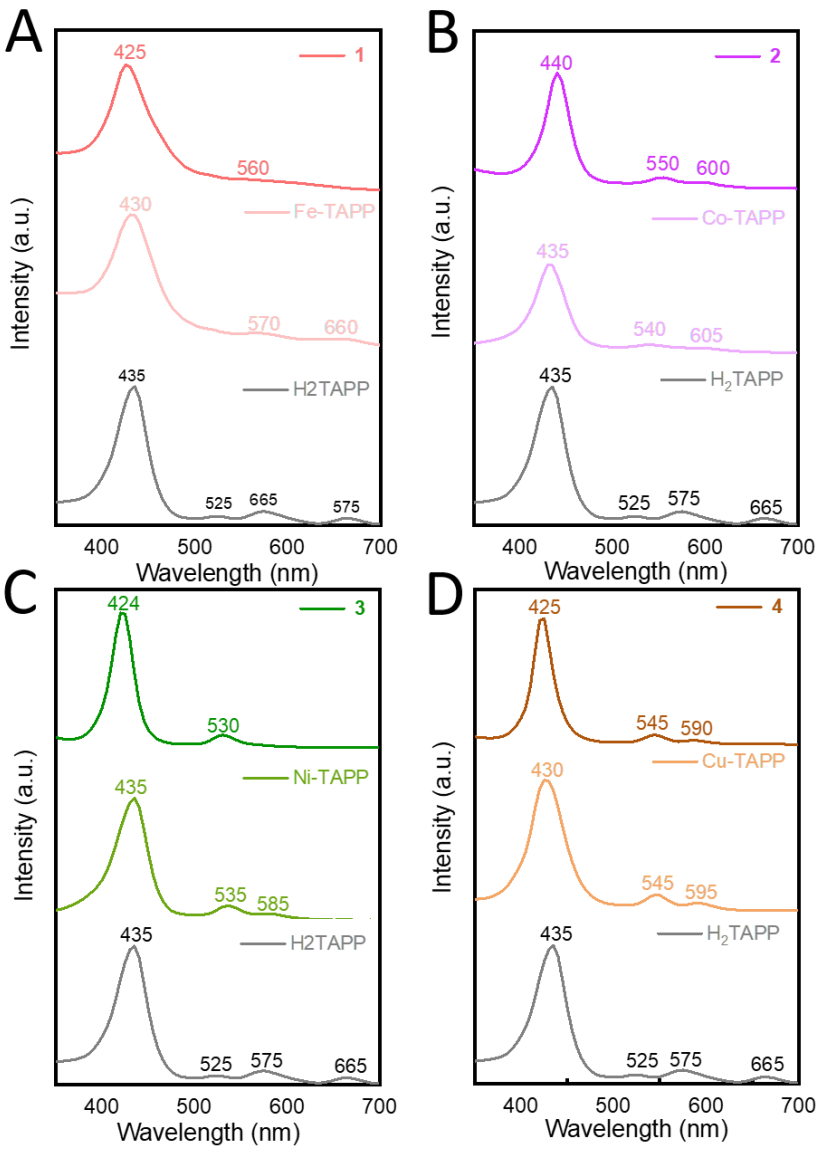

Figure S8: UV-vis spectra of free base porphyrin, metalleted porphyrin and metal porphvlar in DMF. A) H_2TAPP, iron porphyrin and iron polymer (**1**); B) H_2TAPP, cobalt porphyrin and cobalt polymer (**2**); C) H_2TAPP, nickel porphyrin and nickel polymer (**3**); D) H_2TAPP, copper porphyrin and copper polymer (**4**).

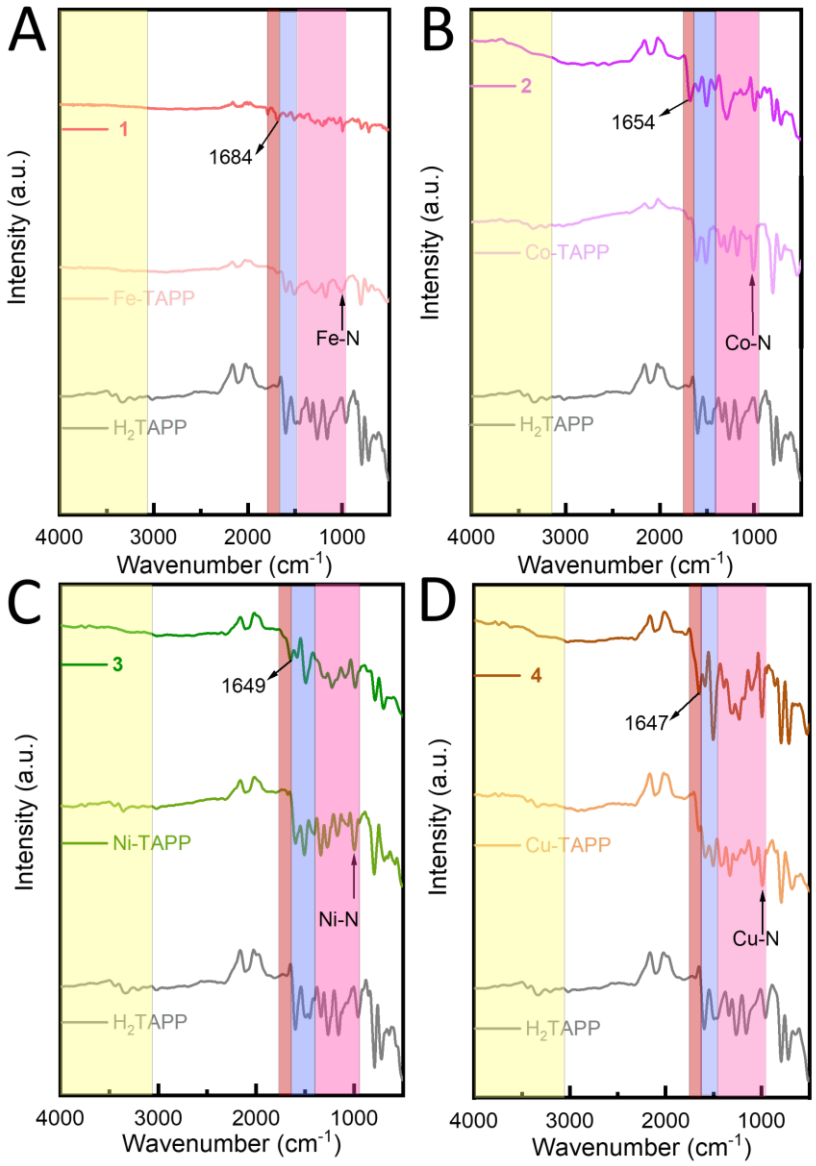

Figure S9. Infrared spectra of the different synthetic stages from meta free to polymerization A) H_2TAPP, iron porphyrin and iron polymer (**1**); B) H_2TAPP, cobalt porphyrin and cobalt polymer (**2**); C) H_2TAPP, nickel porphyrin and nickel polymer (**3**); D) H_2TAPP, copper porphyrin and copper polymer (**4**).

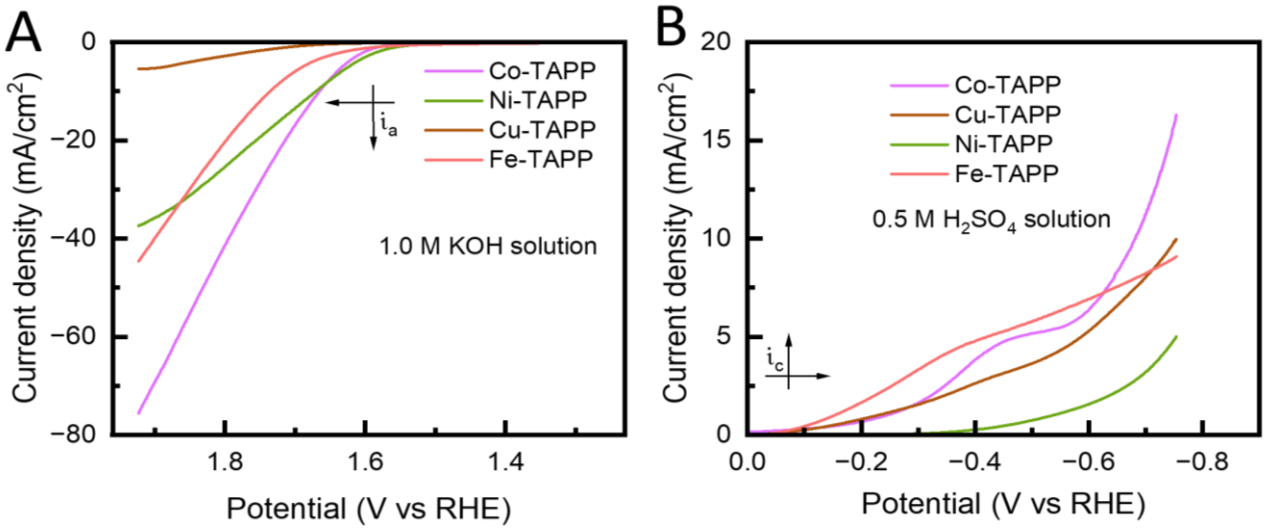

Figure S10. Liner sweep voltammogram of metal porphyrin monomers A) OER and B) HER of co-porphvlar, Ni-porphvlar and Cu-porphvlar voltammogram of metal porphyrin monomers A) OER of co-TAPP, Ni-TAPP and Cu-TAPP B) HER of Co-TAPP, Ni-TAPP and Cu-TAP and C) and D) respective tafel slopes

Table S1. Over potential values of metalloporphyrins

	OER			**HER**		
M-TAPP	η_1	η_{10}	j_{max}	η_1	η_{10}	j_{max}
Fe-TAPP	357	506	-44.6	153	754	9.06
Co-TAPP	357	436	-75.6	229	695	16.3
Ni-TAPP	326	441	-37.4	556	754	5.01
Cu-TAPP	481	693	-5.39	230	754	9.96

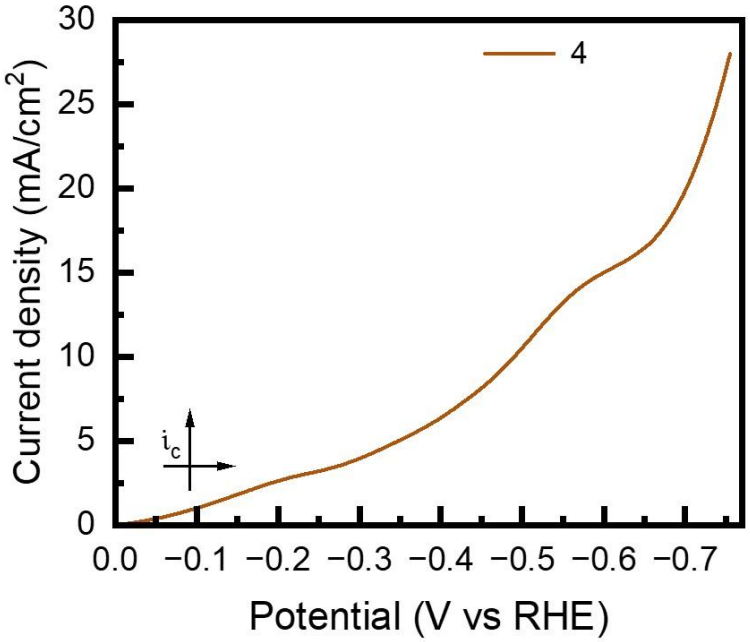

Figure S11: Cathodic linear sweep voltammogram measured in 0.5 M H_2SO_4 solution using copper polymer **4** as HER cathode and cobalt polymer **2** as OER anode pairs in a full cell device experiment.

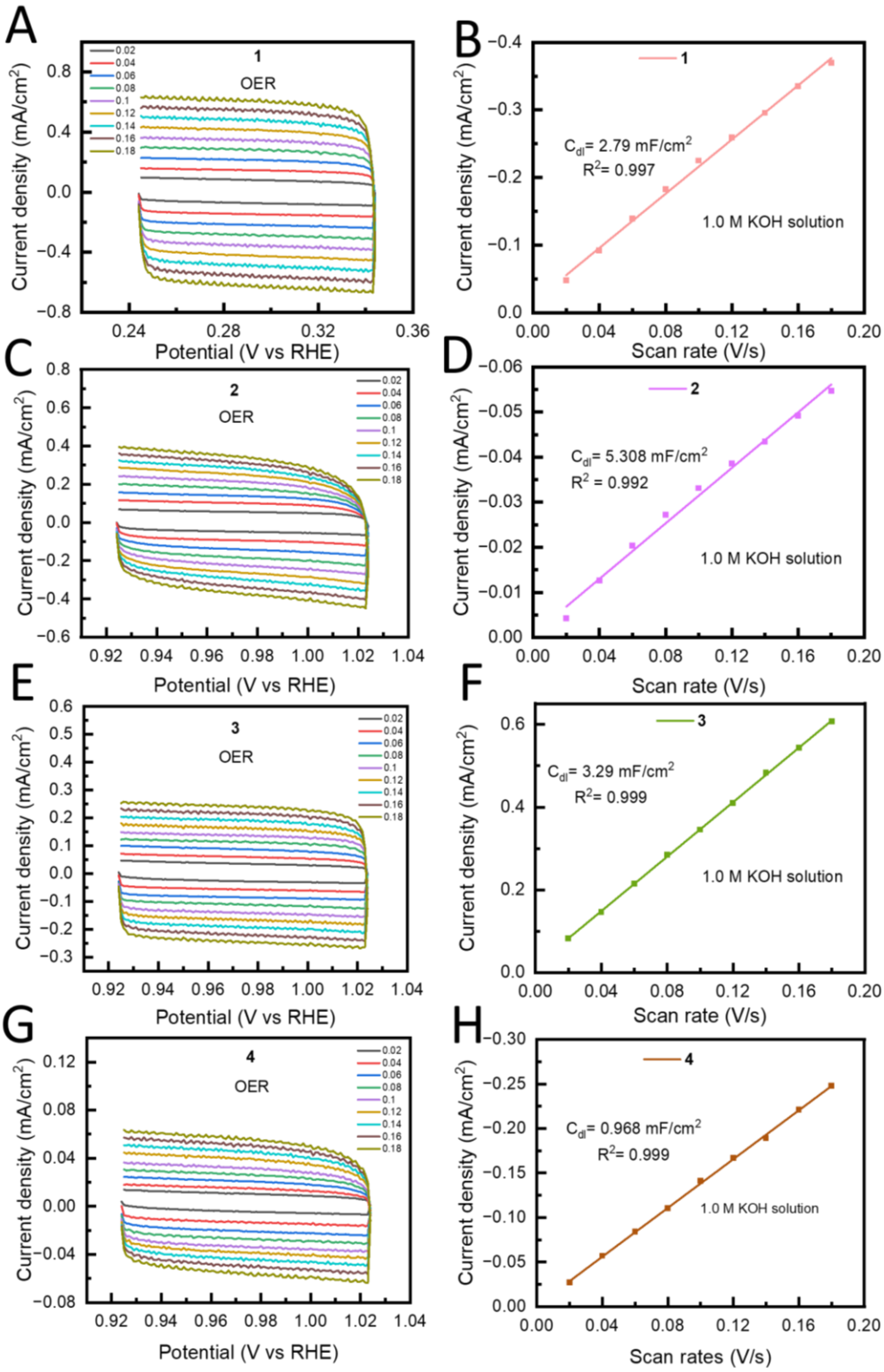

Figure S12. Double layer capacitance of the non-faradaic region in basic conditions.

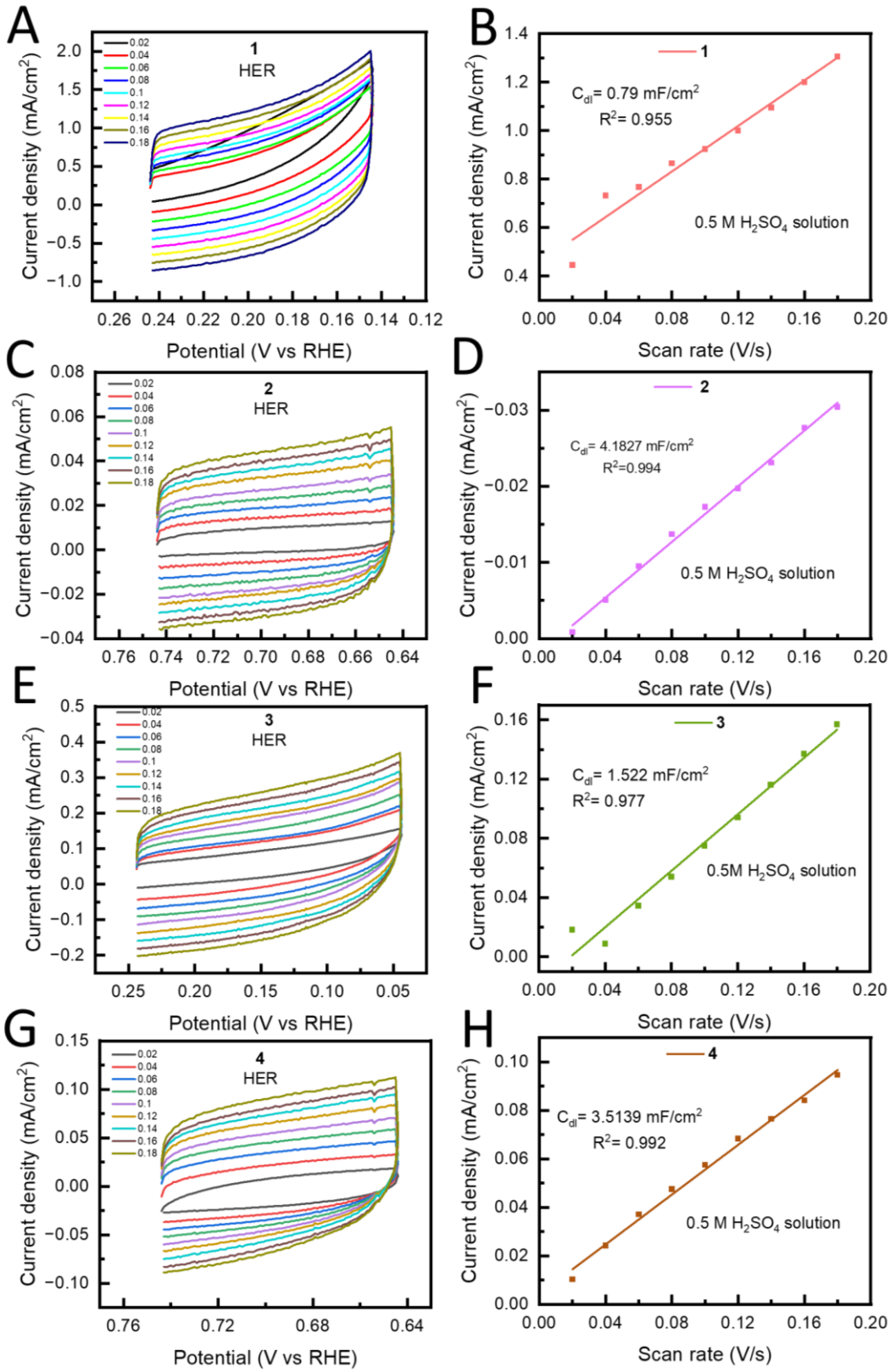

Figure S13. Double layer capacitance of the non-faradaic region in acidic conditions.

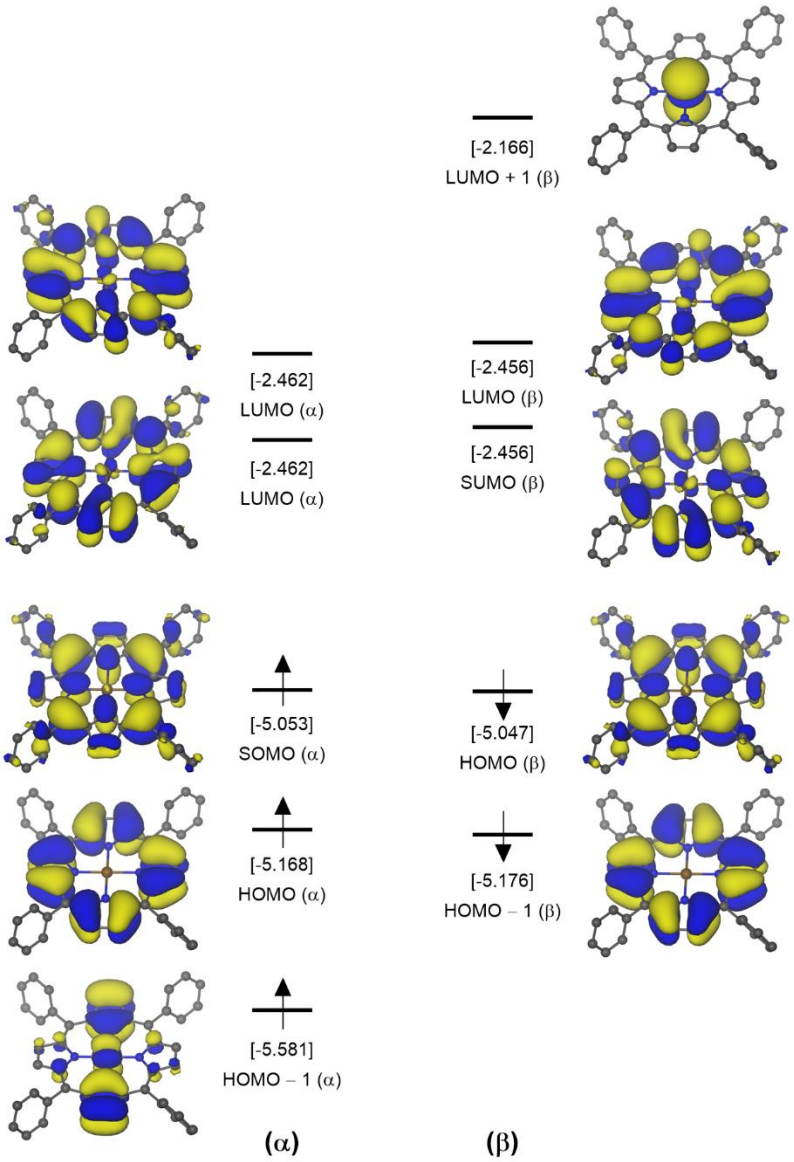

Figure S14. Computed electronic structure of CoTPP at the TPSSh-D3/def2-TZVP level of theory. Molecular orbitals are plotted at an isosurface of 0.02 a.u. Hydrogen atoms are omitted for clarity.

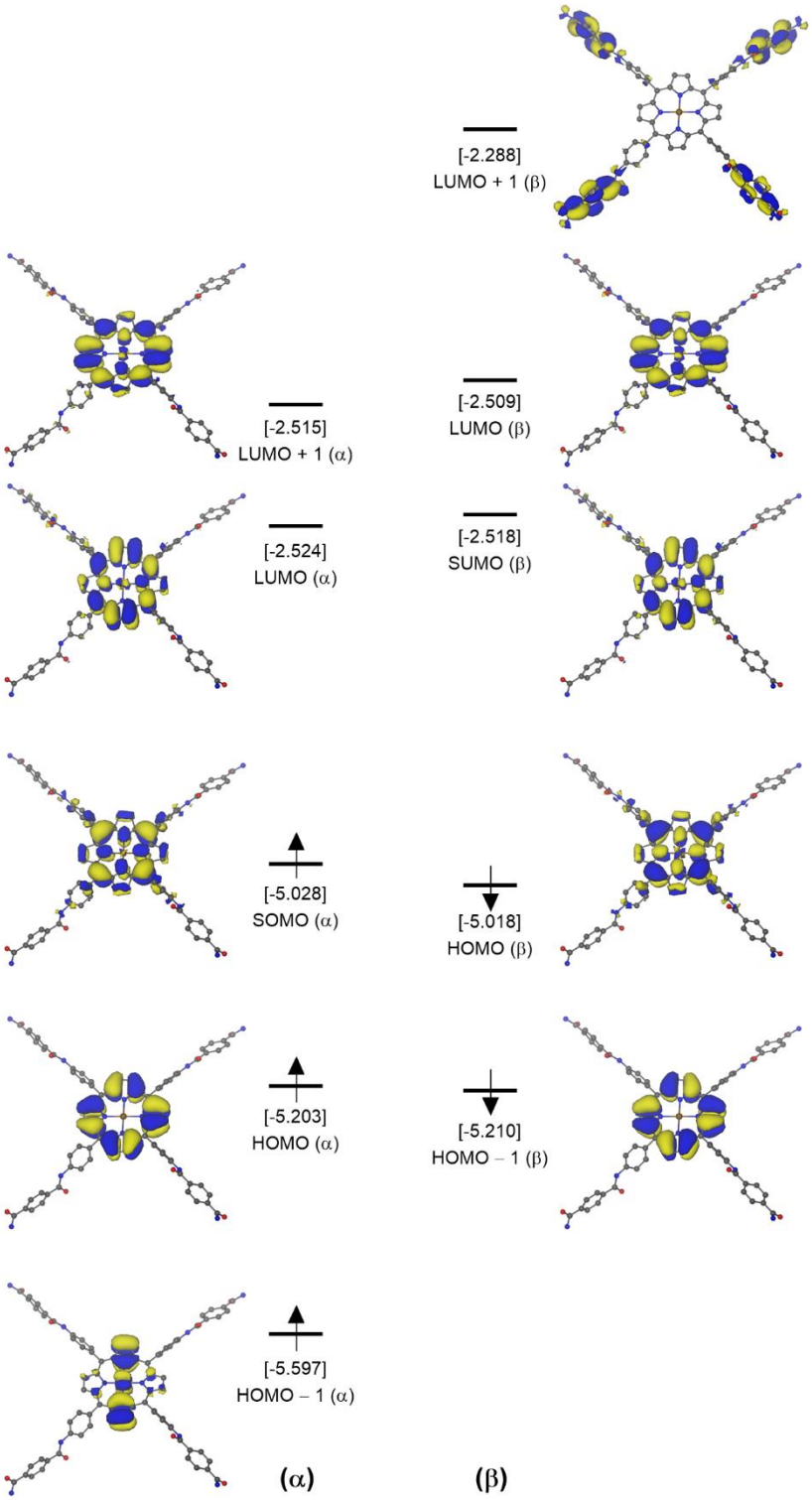

Figure S15. Computed electronic structure of the monomer model of Co-polymer (**2**) at the TPSSh-D3/def2-TZVP level of theory. Molecular orbitals are plotted at an isosurface of 0.02 a.u. Hydrogen atoms are omitted for clarity.

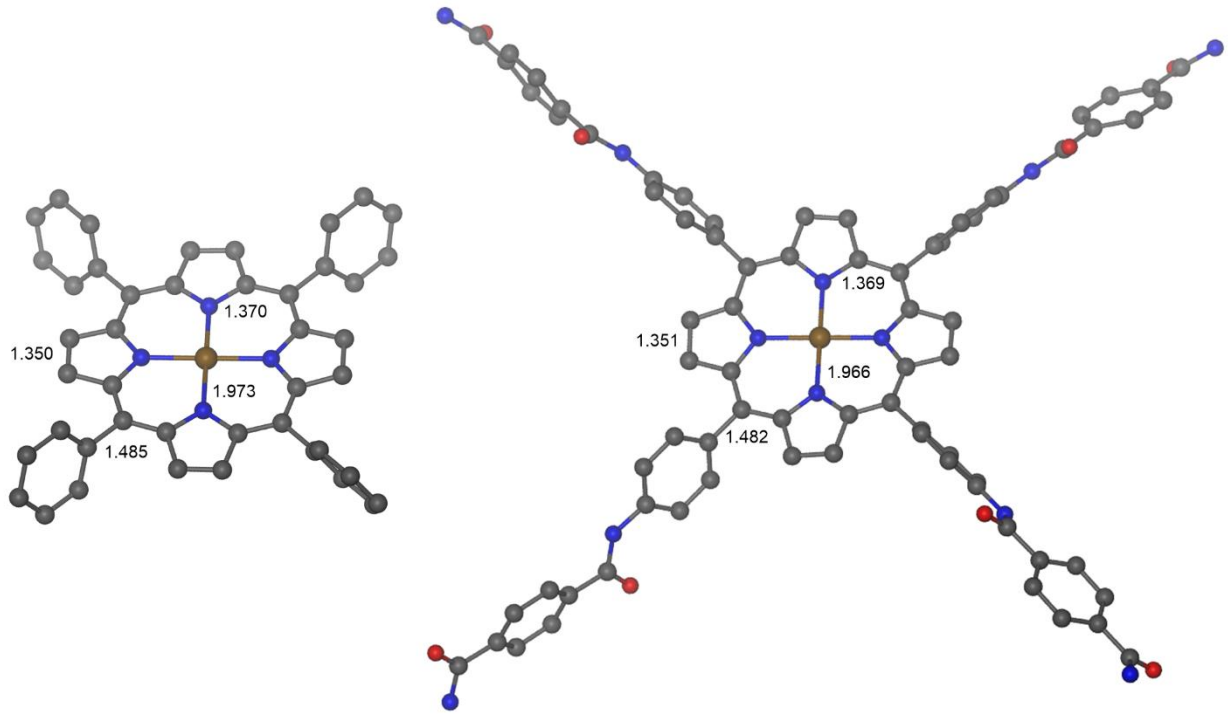

Figure S16. Computed equilibrium structure of CoTPP and the monomer model of Co-polymer (**2**) at the PBE0-D3/ def2-TZVP(-f) level. Calculated metrics are provided in Å. Hydrogen atoms are omitted for clarity.

Table S4. Calculated Mulliken and atomic dipole corrected Hirshfeld atomic charges (TPSSh-D3/def2-TZVP)

CoTPP	**Mulliken**	**Hirshfeld (ADCH)**
Co	0.004	0.216
N	-0.177	-0.145
N	-0.177	-0.146
N	-0.179	-0.139
N	-0.178	-0.142
Co(II) monomer model	**Mulliken**	**Hirshfeld (ADCH)**
Co	0.001	0.202
N	-0.175	-0.107
N	-0.178	-0.148
N	-0.174	-0.124
N	-0.176	-0.131

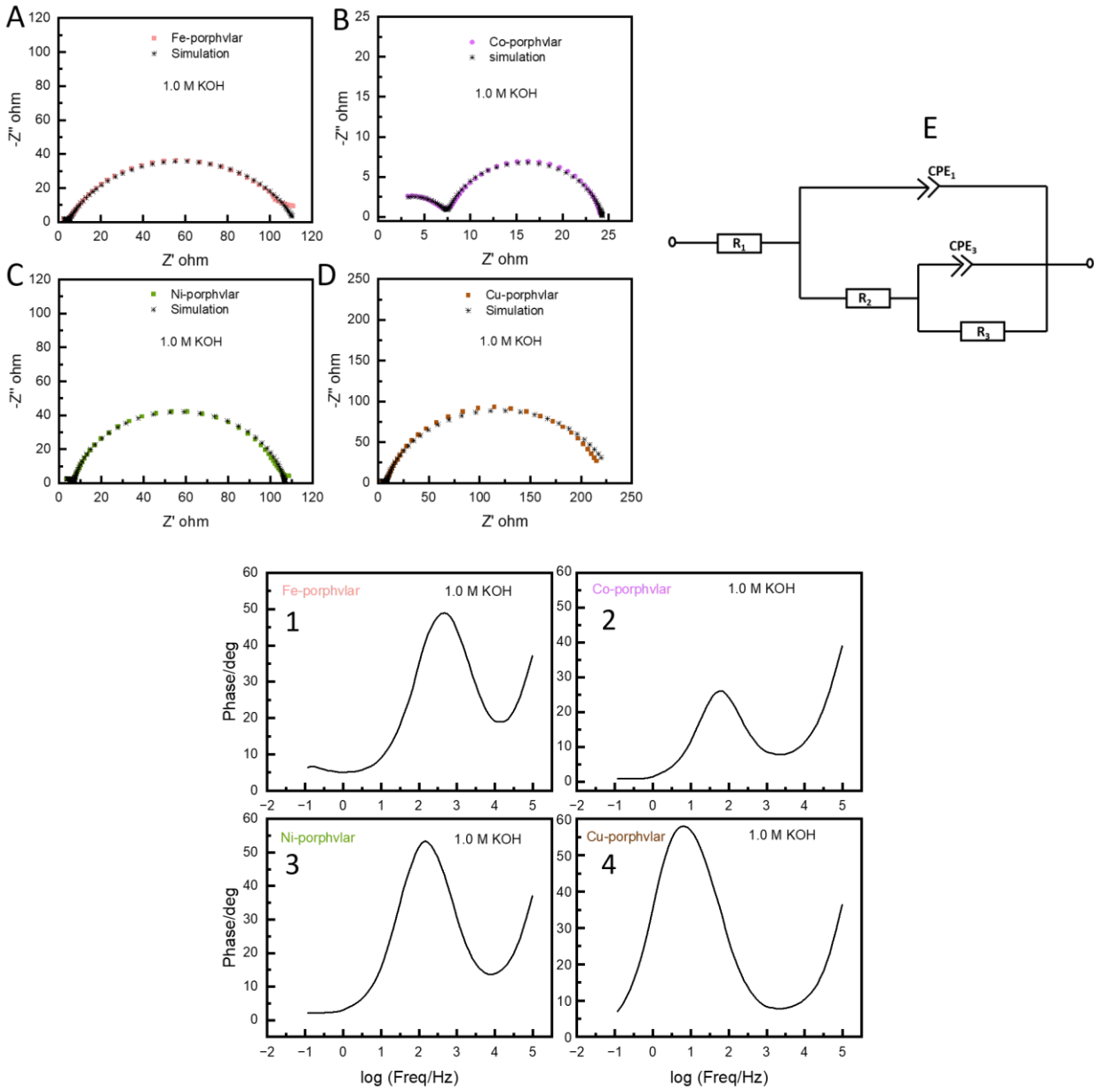

Figure S17. Electrochemical impedance spectroscopy (EIS) of oxygen evolution reaction (OER) in basic condition (1.0 M KOH solutiom) and respective simulation catalyzed by A) Co-porphvlar B) Fe-porphvlar C) Ni-porphvlar and D) Cu-porphvlar. E) the equivalent circuit from simulated impedance spectra. Bode plots of OER in 1.0 M KOH (1) Co-porphvlar (2) Fe-porphvlar (3) Ni-porphvlar and (4) Cu-porphvlar.

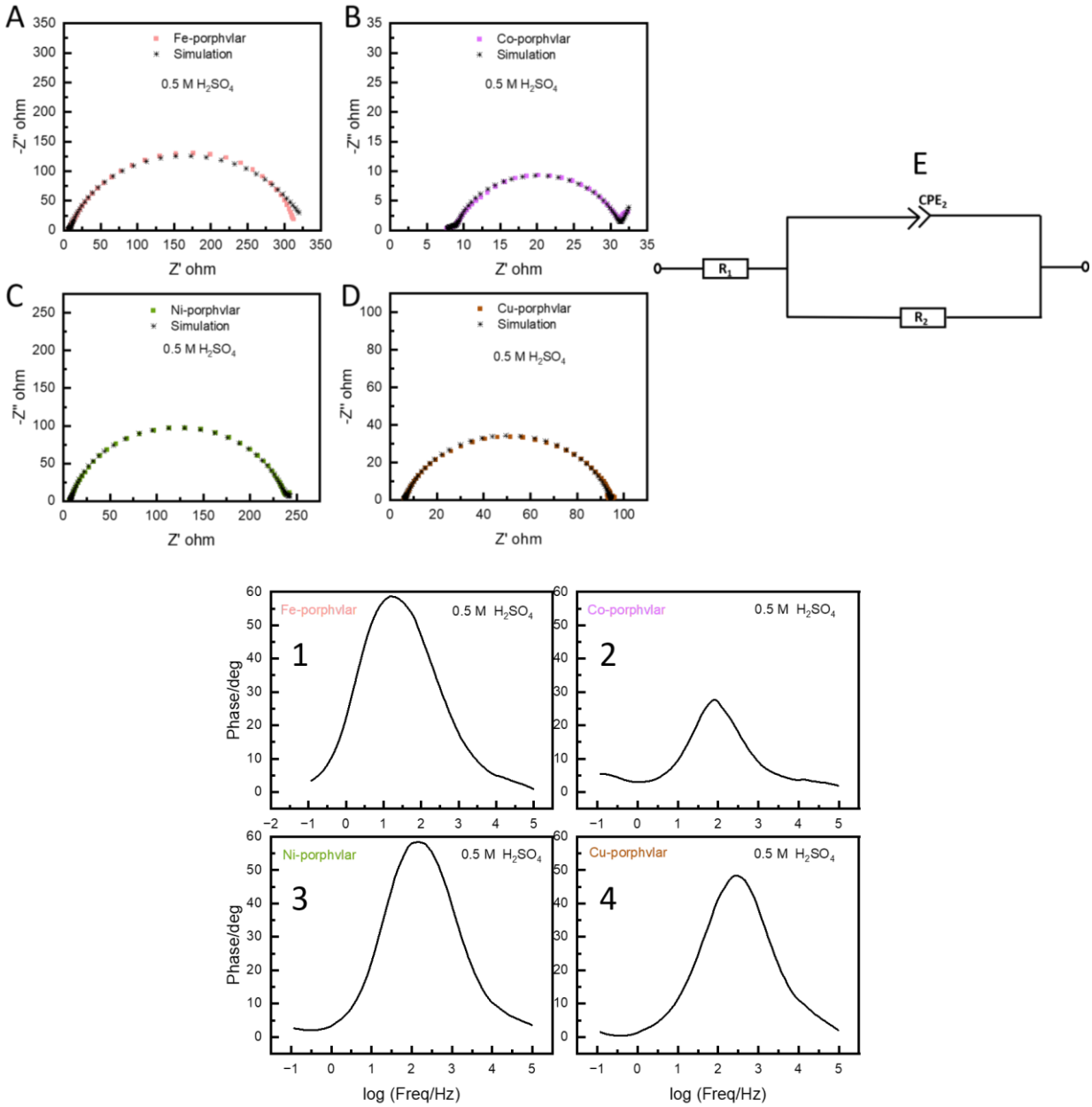

Figure S18 Electrochemical impedance spectroscopy (EIS) of hydrogen evolution reaction (OER) in basic condition (0.5 M H_2SO_4 solution) and respective simulation catalyzed by A) Co-porphvlar B) Fe-porphvlar C) Ni-porphvlar and D) Cu-porphvla. E) the equivalent circuit from simulated impedance spectra. Bode plots of OER in 1.0 M KOH (1) Co-porphvlar (2) Fe-porphvlar (3) Ni-porphvlar and (4) Cu-porphvlar.

Table S2. Equivalent circuits parameters for the oxygen evolution reaction.

	OER			
	Fe-porphvlar	**Co-porphvlar**	**Ni-porphvlar**	**Cu-porphvlar**
R1 (Ohm)	$62.76e^{-15}$	$47.33e^{-15}$	$0.109e^{-12}$	$15.81e^{-15}$
CPE1 ($F{\cdot}s^{(a-1)}$)	$6.529e^{-6}$	$8.08e^{-6}$	$4.84e^{-6}$	$18.52e^{-6}$
A1	0.767	0.742	0.772	0.671
R2 (Ohm)	4.721	7.626	7.238	7.709
CPE3 ($F{\cdot}s^{(a-1)}$)	$0.396e^{-3}$	$0.589e^{-3}$	$82.13e^{-6}$	$0.876e^{-3}$
A3	0.747	0.863	0.893	0.854
R3 (Ohm)	107.2	16.69	99.7	224.5
$\chi/N^{1/2}$	1.641	0.166	1.425	2.866
χ^2	0.02891	0.01577	0.0263	0.09729

Table S3. Equivalent circuits parameters for the hydrogen evolution reaction.

	HER			
	Fe-porphvlar	**Co-porphvlar**	**Ni-porphvlar**	**Cu-porphvlar**
R1 (Ohm)	5.024	7.71	5.567	$21.56e^{-12}$
R2 (Ohm)	303.8	1.847	222.4	86.58
CPE2 (Ohm)	$0.33e^{-3}$	$0.234e^{-3}$	$49.95e^{-6}$	$80.7e^{-6}$
A2	0.8627	0.8974	0.9041	0.8474
CPE3 ($F{\cdot}s^{(a-1)}$)	0.0558	0.3215	0.0667	0.1217
A3	0.253	0.798	0.1913	0.02612
$\chi/N^{1/2}$	5.004	0.2873	1.52	0.9102
χ^2	0.04413	0.01818	0.01624	0.02052

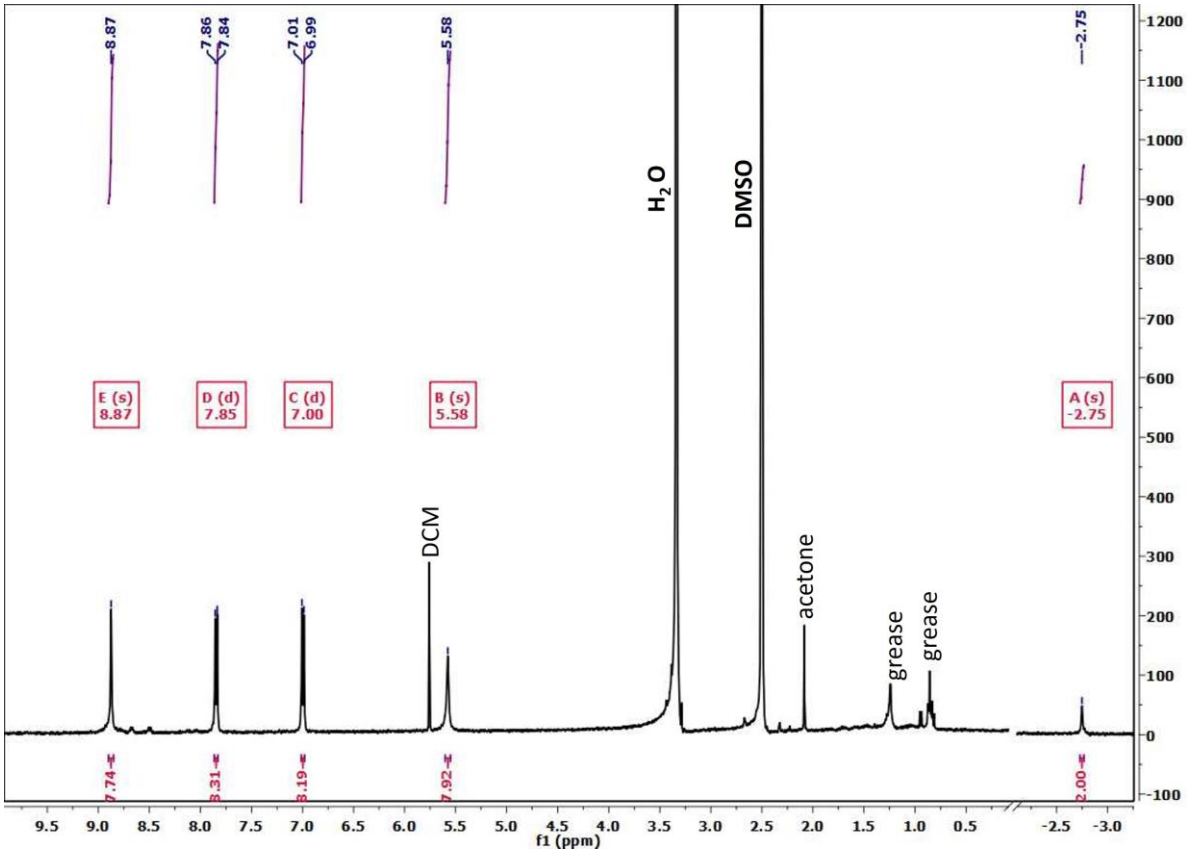

Figure S19. NMR of free base porphyrin (H_2TAPP) in dimethylsulfoxide (DMSO).

Table S5. Comparison of porphyrin material for electrochemical OER

	OER	
Catalyst	**η_{10} (mV)**	**Tafel slope mV/dec**
Fe-porphvlar *	506	195.7
Co-porphvlar *	435	69.2
Ni-porphvlar *	424	96
CoTcPP/ZrP[1]	476	76.4
FeTAPP-NiTCPP-POP[2]	338	52
CoP-2ph-CMP-800[3]	370	86
Fe(Salen)@PIZA-1-400[4]	340	56
TiCP-PCP[5]	310	117
Mn_2DP-a|ITO[6]	470	90
(CoP)n-MWCNTs[7]	430	60.8
PCOF-1-Co[8]	386	89

*This work

Table S6. Comparison of porphyrin material for electrochemical OER

	HER	
Catalyst	**η_{10} mV**	**tafel slope mV/dec**
Fe-porphvlar *	678	363
Co-porphvlar *	437	195
Ni-porphvlar *	644	345
Cu-porphvlar *	436	236
CoCOP[9]	310	161
NiTIPP@CNT[10]	450	104
FeTPP@NiTPP/NF[11]	170	172.4
CoPor-GDY[12]	308	129
CuPor-based CMPs[13]	350	135
TiCP-PCP[5]	339	142

*This work

References

(1) Barraza Alvarez, I.; Wu, Y.; Sanchez, J.; Ge, Y.; Ramos-Garcés, M. V.; Chu, T.; Jaramillo, T. F.; Colón, J. L.; Villagrán, D. Cobalt Porphyrin Intercalation into Zirconium Phosphate Layers for Electrochemical Water Oxidation. *Sustain. Energy Fuels* **2021**, *5* (2), 430–437. https://doi.org/10.1039/d0se01134g.

(2) Meng, J.; Xu, Z.; Li, H.; James Young, D.; Hu, C.; Yang, Y. Porphyrin-based NiFe Porous Organic Polymer Catalysts for the Oxygen Evolution Reaction. *ChemCatChem* **2021**, *13* (5), 1396–1402. https://doi.org/10.1002/cctc.202001876.

(3) Jia, H.; Yao, Y.; Gao, Y.; Lu, D.; Du, P. Pyrolyzed Cobalt Porphyrin-Based Conjugated Mesoporous Polymers as Bifunctional Catalysts for Hydrogen Production and Oxygen Evolution in Water. *Chem. Commun.* **2016**, *52* (92), 13483–13486. https://doi.org/10.1039/c6cc06972j.

(4) Mirza, S.; Chen, H.; Chen, S.-M.; Gu, Z.-G.; Zhang, J. Insight into Fe(Salen) Encapsulated Co-Porphyrin Framework Derived Thin Film for Efficient Oxygen Evolution Reaction. *Cryst. Growth Des.* **2018**, *18* (11), 7150–7157. https://doi.org/10.1021/acs.cgd.8b01300.

(5) Wang, A.; Cheng, L.; Shen, X.; Zhu, W.; Li, L. Mechanistic Insight on Porphyrin Based Porous Titanium Coordination Polymer as Efficient Bifunctional Electrocatalyst for Hydrogen and Oxygen Evolution Reactions. *Dyes Pigments* **2020**, *181*, 108568. https://doi.org/10.1016/j.dyepig.2020.108568.

(6) Mohamed, E. A.; Zahran, Z. N.; Naruta, Y. Covalent Bonds Immobilization of Cofacial Mn Porphyrin Dimers on an ITO Electrode for Efficient Water Oxidation in Aqueous Solutions. *J. Catal.* **2017**, *352*, 293–299. https://doi.org/10.1016/j.jcat.2017.05.018.

(7) Jia, H.; Sun, Z.; Jiang, D.; Du, P. Covalent Cobalt Porphyrin Framework on Multiwalled Carbon Nanotubes for Efficient Water Oxidation at Low Overpotential. *Chem. Mater.* **2015**, *27* (13), 4586–4593. https://doi.org/10.1021/acs.chemmater.5b00882.

(8) Liu, Y.; Yan, X.; Li, T.; Zhang, W.-D.; Fu, Q.-T.; Lu, H.-S.; Wang, X.; Gu, Z.-G. Three-Dimensional Porphyrin-Based Covalent Organic Frameworks with Tetrahedral Building Blocks for Single-Site Catalysis. *New J. Chem.* **2019**, *43* (43), 16907–16914. https://doi.org/10.1039/C9NJ04017J.

(9) Wang, A.; Cheng, L.; Zhao, W.; Shen, X.; Zhu, W. Electrochemical Hydrogen and Oxygen Evolution Reactions from a Cobalt-Porphyrin-Based Covalent Organic Polymer. *J. Colloid Interface Sci.* **2020**, *579*, 598–606. https://doi.org/10.1016/j.jcis.2020.06.109.

(10) Wang, Y.; Song, D.; Li, J.; Shi, Q.; Zhao, J.; Hu, Y.; Zeng, F.; Wang, N. Covalent Metalloporphyrin Polymer Coated on Carbon Nanotubes as Bifunctional Electrocatalysts for Water Splitting. *Inorg. Chem.* **2022**, *61* (26), 10198–10204. https://doi.org/10.1021/acs.inorgchem.2c01415.

(11) Yuan, S.; Cui, L.; He, X.; Zhang, W.; Asefa, T. Nickel Foam-Supported Fe,Ni-Polyporphyrin Microparticles: Efficient Bifunctional Catalysts for Overall Water Splitting in Alkaline Media. *Int. J. Hydrog. Energy* **2020**, *45* (53), 28860–28869. https://doi.org/10.1016/j.ijhydene.2020.08.013.

(12) Pan, Q.; Chen, X.; Liu, H.; Gan, W.; Ding, N.; Zhao, Y. Crystalline Porphyrin-Based Graphdiyne for Electrochemical Hydrogen and Oxygen Evolution Reactions. *Mater. Chem. Front.* **2021**, *5* (12), 4596–4603. https://doi.org/10.1039/D1QM00285F.

(13) Cui, S.; Qian, M.; Liu, X.; Sun, Z.; Du, P. A Copper Porphyrin-Based Conjugated Mesoporous Polymer-Derived Bifunctional Electrocatalyst for Hydrogen and Oxygen Evolution. *ChemSusChem* **2016**, *9* (17), 2365–2373. https://doi.org/10.1002/cssc.201600452.